

EFFECTS OF FOREIGN OBJECT DAMAGE (FOD) ON THE FATIGUE LIMIT STRENGTH OF Ti-6Al-4V

T. Nicholas¹, S.R. Thompson², W.J. Porter³ & D.J. Buchanan³

¹Air Force Institute of Technology (AFIT/ENY), Wright-Patterson AFB, OH 45433, USA

²Air Force Research Laboratory, Materials and Manufacturing Directorate,
Wright-Patterson AFB, OH 45433, USA

³University of Dayton Research Institute, Dayton, OH 45469

ABSTRACT

To shed light on the FOD resistance of a titanium alloy, a comprehensive series of experiments under very controlled conditions has been carried out. Steel spheres, 3.18 mm in diameter, were impacted normally at velocities of 200 or 300 m/s onto 3.18 mm thick flat plates of Ti-6Al-4V forged plate. The plate specimens were then fatigue tested in either tension, bending, or torsion using a step-loading technique to determine the fatigue strength at 10^6 cycles. Half of the specimens were stress relief annealed in order to eliminate any residual stresses and to be able to sort out the effects of residual stresses on the fatigue limit strength. To further understand the role of impact and the dynamic behavior of the material, damage was imparted to the material in the form of either a quasi-static ball indentation or the low velocity impact of a ball using a pendulum to the identical depths as obtained in the ballistic experiments. Elastic stress concentration factors, k_t , were computed using a FEM simulation of the geometry corresponding to the two nominal impact depths of 0.22 or 0.41 mm. Experimental values of the fatigue notch factor and k_f were compared for the different methods of imparting damage as well as for the different loading conditions (tension, torsion, or bending). Fractography was conducted on selected samples to locate the fatigue origin and to relate this to k_t at a given location, taking into account the residual stresses imparted during any of the impact or indent procedures. This large body of data has been sorted to help quantify and explain the relative contributions of the critical parameters involved in FOD.

1 INTRODUCTION

Foreign objects ingested into rotating components in a gas turbine engine can cause a severe degradation of the fatigue properties of the impacted materials. Objects such as sand, small stones, and other debris can cause dents, nicks, tears, or cracks that, in turn, reduce the fatigue capability of the material. Several factors have to be considered when evaluating the residual fatigue strength of an impacted material. First is the geometry of the impact damage such as the shape or stress concentration of a crater or dent. Second, the role of residual stresses imparted to the material during the impact event should be determined. Third, actual damage in terms of cracking or other microstructural damage has to be considered. While attempts have been made in previous research to sort out the role of these factors, the variability in damage from ballistic impacts of small hard particles on blade leading edge geometries has tended to obscure any specific conclusions on the role of each mechanism. Ruschau et al. [1] have investigated the FOD resistance of simulated airfoil geometry of the Ti-6Al-4V alloy used herein under ballistic as well as simulated impact conditions. Peters et al. [2] have investigated the ballistic impact damage on the same alloy in a flat plate geometry under normal impact and tensile fatigue loading. This investigation extends the

study of FOD to a wide range of test conditions involving axial, torsion, and bending loads as well as using stress relief annealing to separate out the role of residual stresses. The conditions chosen for the current investigation include those found to impart deformation only as well as microcracking under ballistic impact (Peters et al. [2]). Because of the simple impact geometry of a flat plate impacted normally, as opposed to impacting a leading edge at a non-zero angle of incidence, the scatter in material behavior was reduced somewhat.

2 EXPERIMENTS

For the ballistic impacts, steel spheres, 3.18 mm in diameter, were impacted normally at velocities of either 200 or 300 m/s onto 3.18 mm thick flat plates of Ti-6Al-4V forged plate material in STOA condition. Half of the specimens were stress relief annealed in order to eliminate any residual stresses and to be able to sort out the effects of residual stresses on the fatigue limit strength. To further understand the role of impact and the dynamic behavior of the material, damage was imparted to the material in the form of either a quasi-static ball indentation or the low velocity impact of a ball using a pendulum to the identical depths as obtained in the ballistic experiments. The pendulum approach or equivalent is sometimes considered to be an equivalent method of imparting ballistic impact damage. In both types of impacts, the ball used for producing the indent was the same diameter as that used in the ballistic impacts. The depth of indent for the quasi-static and pendulum indents was chosen to be the same as the average value for the ballistic impacts, 0.22 and 0.41 mm, for the 200 and 300 m/s impacts, respectively. As in the case of the ballistic impacts, stress relief annealing was used on half of the quasi-static and pendulum impact specimens. All of the plate specimens were then fatigue tested in tension, bending, or torsion using a step-loading technique. This involves testing at a stress level below the anticipated fatigue limit stress to 10^6 cycles before the load was increased. The procedure is continued until failure occurs on the last cycle block.

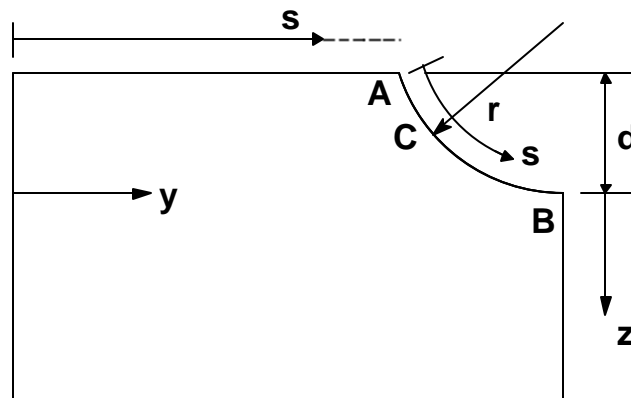


Figure 1. Geometry of half cross section through middle of notch.

3 ANALYSIS

The elastic stress concentration factor was determined for the two notch geometries from a finite element simulation of the rectangular test specimens. The depth of indent for the notch geometry was 0.22 and 0.41 mm for the shallow and deep notches, respectively. It was assumed throughout that the notch has a spherical surface whose radius is half of the impacting sphere whose diameter was 3.18 mm. The finite element model used to calculate elastic stress concentration factors, k_t ,

used the geometry and coordinate system shown in Fig. 1 for half the cross section through the middle of the notch. The commercial finite element code, ANSYS, was employed for all analyses. Twenty-node solid brick elements were selected to accurately model the spherical surface. These higher-order elements are more appropriate for capturing the stress gradients at the notch. Mesh refinement in the vicinity of the notch was performed to determine the accuracy of the stress concentration factor. Final element size in the vicinity of the notch was approximately 0.020 mm.

The results for the axial stresses due to an average axial stress of 100 MPa and a bending moment that causes 100 MPa along the surface are presented in Figs 2 and 3 for stresses along the coordinates s and z , respectively, as denoted in Fig. 1. Since the s coordinate is measured along the surface of the cross section, the center of the notch corresponding to $y = 5$ mm (10 mm wide plate), is located at $s = 5.039$ and $s = 5.102$ mm in the figures for the shallow and deep notches, respectively. Similarly, the coordinates for the point A in Fig. 1, where the notch intersects the surface of the plate, are $s = 4.201$ and $s = 3.939$ mm for the shallow and deep notches, respectively. These locations are shown as the edge of notch (EON) in Fig. 2 as dotted lines. Values of k_t are summarized for the two notch sizes in axial tension and pure bending in Table 1. For most cases, the locations for the maximum value of the local stress concentration are at A along the surface at the edge of the notch and B at the root of the notch, the latter having the larger k_t in most cases. However, for the deep (large) notch under bending, the maximum value of k_t (1.39) occurs at point C at the interior of the notch and is slightly higher than the value at point B at the bottom of the notch where $k_t = 1.36$.

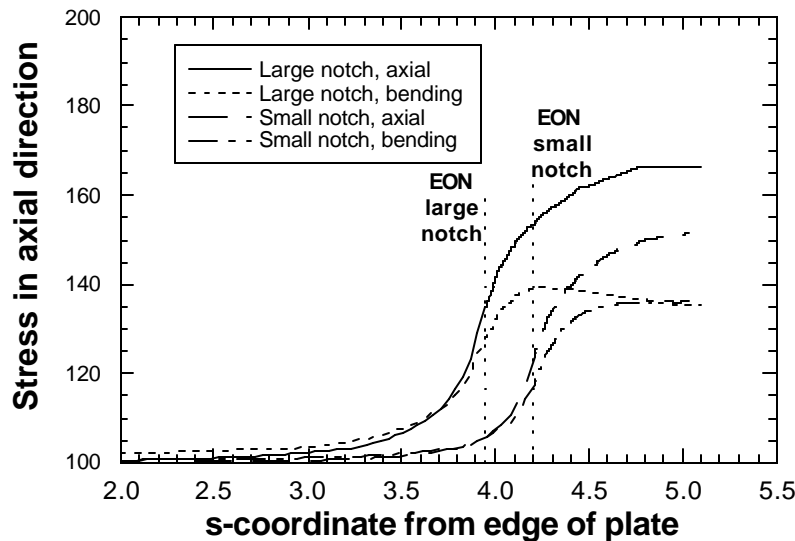


Figure 2. Stress distribution along surface of plate with indent.

In addition to the values of k_t , the stress gradient also has to be considered. Along the surface, Fig. 2 illustrates that the stresses decay in a slow and smooth manner as a function of distance from the peak value at location A. On the other hand, the rate of decay from point B at the root of the notch is much steeper as shown in Fig. 3. Both figures are drawn to the same vertical (stress) scale and nearly the same horizontal (distance) scale, so a comparison of stress gradients can be easily made. In Fig. 3, the two curves for the cases of bending in the small and large notch are almost identical and plot on top of each other. From Fig. 2, the size of the notch can be readily

seen as measured along the s axis going from the dotted line to the end of the curve drawn. The gradients going into the depth, shown in Fig. 3, are much steeper than what is normally observed for 2-d notch geometries of the same relative dimensions. This is due to a combination of the 3-d nature of the problem as well as the use of bending in some of the computations which creates an additional stress gradient through the depth.

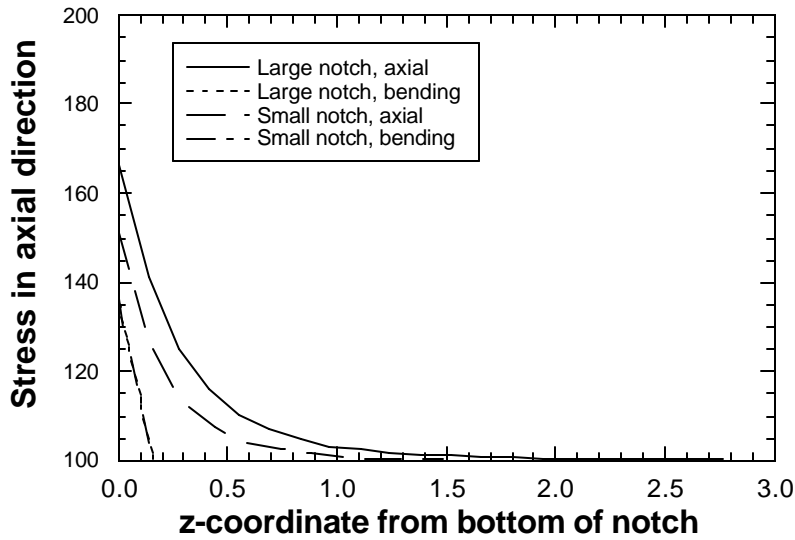


Figure 3. Stress distribution into depth below notch.

Table 1. Computed values of k_t for notches (* $s = 4.26$ mm).

	Small notch		Large notch		
	Bottom	Surface	Bottom	Surface	Other
Axial	1.51	1.24	1.67	1.35	
Bending	1.36	1.18	1.36	1.28	1.39*

Table 2. Experimental values of k_f for notches under tension, $R = 0.1$.

Notch type	Ballistic	Pendulum	Quasi-static
AR Shallow	1.31	1.20	1.19
AR Deep	1.69	1.31	1.26
SR Shallow	1.26	1.10	1.07
SR Deep	1.53	1.11	1.09

4. RESULTS AND DISCUSSION

The fatigue limit stress, σ_{FLS} , corresponding to a life of 10^6 cycles was determined from step tests using the interpolation formula

$$\sigma_{FLS} = \sigma_{prior} + \Delta\sigma (N_f/10^6) \quad (1)$$

where σ_{prior} is the stress in the cycle block prior to failure, N_f is the number of cycles in the last block where failure occurs, and $\Delta\sigma$ is the stress increment going from the prior block to the last block. For each value of σ_{FLS} , the fatigue notch factor, k_f , was calculated from the definition

$$k_f = \text{smooth bar FLS/notched FLS} \quad (2)$$

The FLS for smooth bar tests on this material at 10^6 cycles was 600 MPa at $R = 0.1$ where all of the tension tests were conducted. The results for the average value of k_f from 2 tests at each of the conditions shown are summarized in Table 2. The symbol “AR” is used to denote as received material, that is, material as tested without stress relief after the indents were put in. The symbol “SR” denotes samples that were stress relieved after indentation. The three types of indentations are represented in this data base for all of the tensile tests conducted at $R = 0.1$. The pendulum impacts were conducted at the necessary velocities around a few m/s to obtain the targeted penetration depths with the mass of the impacting fixture. The results of all of the tensile fatigue tests show that stress relief (SR) improved the fatigue strength in all cases, although the improvement was not very large. This implies that some tensile residual stresses were present after all of the indentation procedures, since nothing changes during the SR process other than the removal of residual stresses. This finding is the same as that reported in Ruschau et al. [1] on similar impact studies on leading edge geometries. Of greater significance in the findings here is the observation that ballistic impacts to the same depth as pendulum or quasi-static indentations are more severe in terms of the resulting fatigue limit strength or notch fatigue factor. This is especially true for the deeper indents corresponding to ballistic impacts at 300 m/s. In the work of Peters et al. [2], the impacts at 300 m/s produced small amounts of cracking at the crater whereas the impacts at 200 m/s produced no observable cracks. From these observations, it is concluded that low velocity (pendulum) or quasi-static indentation does not produce the same amount of damage as ballistic impact even though the resulting craters are of the same dimension. This finding is supported by similar findings by Ruschau et al. [1] and by more recent unpublished results from the same group.

REFERENCES

- [1] Ruschau, J., Thompson, S.R. and Nicholas, T., “High Cycle Fatigue Limit Stresses for Airfoils Subjected to Foreign Object Damage,” *Int. J. Fatigue*, Vol. 25, pp. 955-962, 2003.
- [2] Peters, J.O., Roder, O., Boyce, B.L., Thompson, A.W. and Ritchie, R.O., “Role of Foreign-Object Damage on Thresholds for High-Cycle Fatigue in Ti-6Al-4V,” *Metal. Mat. Trans.*, Vol. 31A, pp. 1571-1583, 2000.